

A 1000-year chironomid-based salinity reconstruction from varved sediments of Sugan Lake, Qaidam Basin, arid Northwest China, and its palaeoclimatic significance

CHEN JianHui¹, CHEN FaHu^{1†}, ZHANG EnLou², BROOKS Stephen J³, ZHOU AiFeng¹ & ZHANG JiaWu¹

¹ MOE Key Laboratory of Western China's Environmental Systems, Lanzhou University, Lanzhou 730000, China;

² State Key Laboratory of Lake Science and Environment, Nanjing Institute of Geography and Limnology, Chinese Academy of Sciences, Nanjing 210008, China;

³ Department of Entomology, Natural History Museum, London SW7 5BD, UK

A 1000-year high-resolution (~10 years) chironomid record from varved sediments of Sugan Lake, Qaidam Basin on the northern Tibetan Plateau, is presented. The chironomid assemblages are mainly composed of the relatively high-saline-water taxa *Psectrocladius barbimanus*-type and *Orthocladius/Cricotopus*, and the relatively low-saline-water taxa *Procladius* and *Psectrocladius sordidellus*-type. Variations in the chironomid fauna and inferred salinities suggest that over the last millennium, the Sugan Lake catchment has alternated between contrasting climatic conditions, having a dry climate during the period 990–1550 AD, a relatively humid climate during the Little Ice Age (LIA) (1550–1840 AD), and a dry climate again from 1840 AD onwards. At the decadal to centennial scale, a wet event around 1200–1230 AD, interrupting the generally arid period (990–1550 AD), and a dry event around 1590–1700 AD, punctuating the generally humid period (1550–1840 AD), are clearly documented. Trends in the chironomid-based salinity time series indicate a highly unstable climate during the LIA when salinity fluctuations were of greater magnitude and higher frequency. The effective moisture evolution in the Sugan Lake catchment during the last millennium reconstructed by chironomid analysis is in broad agreement with previous palaeo-moisture data derived from other sites in arid Northwest China (ANC). The LIA, characterized by generally humid conditions over the westerly-dominated ANC was distinctly different from that in monsoonal China, implying an “out-of-phase” relationship between moisture evolution in these two regions during the past 1000 years.

Sugan Lake, arid Northwest China, sub-fossil chironomid, effective moisture, last millennium

High-quality palaeoclimate data are essential for understanding climate variability, and provide the requisite background knowledge for increasing the reliability of climate models^[1]. Arid Northwest China (ANC), located in the innermost center (35°–50°N, 75°–105°E) of the Eurasian continent, is of considerable significance with regard to regional responses to global climatic change. Chen et al.^[2] have recently proposed an “out-of-phase” relationship between the evolution of Holocene moisture

in ANC and the monsoonal region of China. Shi et al.^[3] have suggested that the climate changed from warm-dry to warm-wet in 1987 in ANC as a consequence of global warming and an enhanced water cycle. It has also been

Received November 18, 2008; accepted February 17, 2009; published online May 27, 2009

doi: 10.1007/s11434-009-0201-8

†Corresponding author (email: fhchen@lzu.edu.cn)

Supported by the Fund for Creative Research Groups, National Natural Science Foundation of China (Grant No. 40721061) and Research Fund for the Doctoral Program of Higher Education (Grant No. 20060730003)

suggested that humid climatic conditions prevailed in this region during the Western and Eastern Han Dynasties (206 BC – 220 AD)^[4], and the Little Ice Age (LIA)^[5]. However, in general, a detailed understanding of moisture variations in ANC over the past millennium has not yet been acquired for lack of well-dated palaeoclimate archives and sensitive climate proxies. The annually laminated sediments of Sugan Lake, a hydrologically-closed saline lake in the northern part of the Qaidam Basin, northern Tibetan Plateau, afforded us a unique opportunity to investigate the moisture evolution in ANC over the last 1000 years at a relatively high resolution, using sub-fossil Chironomidae (Insecta: Diptera) as an indicator of past water salinity.

In the last two decades, chironomids have been increasingly used and recognized as sensitive indicators of past climatic and environmental change^[6]. As in other Diptera, chironomids have four life stages: egg, larva, pupa and adult. The chitinous head capsules of the 3rd and 4th instar aquatic larvae are usually well-preserved in lake sediments, and can be identified to at least generic level^[7]. There are several key attributes that make chironomids suitable as environmental indicators. They are ubiquitous, abundant, species-rich (a total of 339 genera, 4147 species of aquatic Chironomidae have been described worldwide^[8]), stenotopic and respond rapidly to environmental change^[9,10]. Temperature is most significant in driving the broad-scale geographic distribution and abundance of chironomids^[9]. Nevertheless, in saline lakes of arid and semiarid regions, chironomid assemblages usually reflect the salt concentration fluctuations within the lake basin^[11]. Given that changing salinity in closed-basin lakes is commonly used as a proxy for effective moisture (precipitation+runoff/evaporation), the chironomid assemblages are thus linked to climate^[12]. Chironomid-based palaeosalinity studies have been carried out in Equatorial Africa^[13–15] and southwestern Canada^[16,17], and the effective moisture changes have been convincingly reconstructed. In China, Zhang et al.^[18] developed the first chironomid-salinity inference model from 38 Tibetan Plateau lakes (including Sugan Lake). Subsequent work further indicated that fossil chironomids could be a sensitive proxy for salinity fluctuations in Sugan Lake at the 50 to 100-year scale^[19]. Here, using the chronological framework provided by varve dating^[20,21], we present a high-resolution (~10 years) chironomid-based salinity reconstruction covering the past millennium from Sugan

Lake, to explore the variability of regional effective moisture in detail.

1 Materials and methods

The Sugan Lake (38°51'N, 93°54'E) is located in Sugan Basin in the northern margin of Qaidam Basin on the northeastern Tibetan Plateau (Figure 1). Most of the Sugan Basin lies between 2800 and 3200 m a.s.l., higher latitudes being located in the southeast rather than the northwest. The catchment, covering an area of 19854 km²^[22], is hyper-arid (annual precipitation 18.7 mm, potential evaporation >2900 mm) and has a mean annual temperature of 2.75°C^[23]. The Sugan Lake is mainly fed by two rivers (Big Harteng River and Small Harteng River), which originate in the high mountains to the southeast, infiltrate into the Gobi-desert zone in the piedmont plains and then either seep out as springs and small surface streams subsequently flowing into the lake, or move downward, recharging the groundwater inflow along the lake shoreline^[24]. The Sugan Lake is a hydrologically closed kidney-shaped lake having a maximum length of 20.9 km, a maximum width of 7.9 km and an area of 103.68 km². The mean depth is 2.84 m and the maximum depth is 6 m^[25]. The lake water chemistry is of the Cl-SO₄-Na-Mg type, with a mean salinity of 31.83 g/L and a conductivity of 27.7 mS/cm^[20].

Several cores were retrieved from various water depths through the frozen lake surface with a piston corer in the winters of 2000 to 2004^[21,23]. The laminated upper 5.5 m of a 7.9 m core (SG03I), taken from a depth of 4.5 m in the central part of the lake, have proved to be varved sediments, based on detailed mineralogical, structural and biological examinations and in comparison to a ²¹⁰Pb chronology on parallel core (SG00E)^[20]. Varve counting was therefore used to establish a chronology extending back to 670 BC^[21]. Chironomid analysis was applied to the upper 3.8 m, spanning 300 AD–2000 AD. However, the chironomid-based salinity reconstruction presented here only covers the last millennium (990 AD–2000 AD, 0–2.7 m). A total of 95 samples were analyzed, with a mean sample interval of ~3 cm, equivalent to a temporal resolution of ~10 years.

Sediments were processed for chironomid analysis according to standard methods^[9,10]: (1) 0.5–4 g freeze-dried subsamples were deflocculated for 5–10 min in

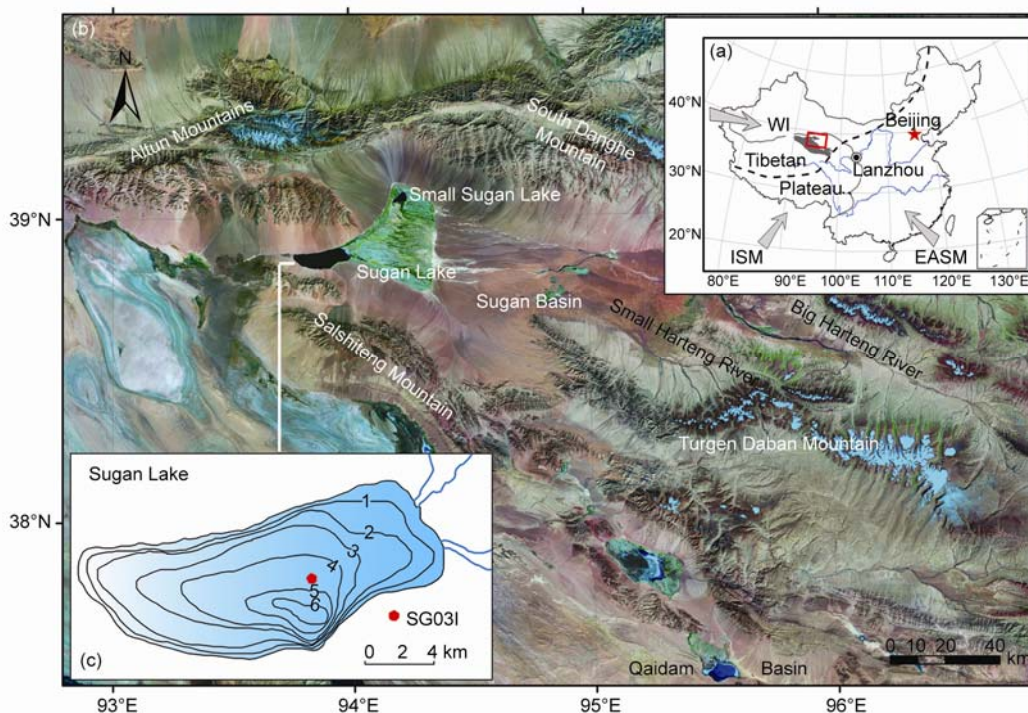


Figure 1 (a) Location of Suga Lake catchment and surrounding area (framed by red), Qaidam Basin (shaded area), northern Tibetan Plateau, China, and the dominant circulation systems of the Westerlies (WI), the Indian summer monsoon (ISM), and the East Asian summer monsoon (EASM). Dashed line indicates modern Asian summer monsoon limit^[26,27]. (b) Landsat ETM satellite image of Suga Lake catchment and surrounding area. (c) Bathymetry of Suga Lake^[20]. Red dot indicates location of core SG031.

10% KOH heated to 75°C; (2) the sediment was passed through 212 and 90 μm mesh sieves; (3) the chironomid head capsules were hand picked a 40× stereo microscope. Given the relatively high carbonate content (~40% on average) of our samples, 5% HCl was used to eliminate the carbonates after the first round of head capsule picking. Step (2) and (3) were subsequently repeated to guarantee that all the chironomid remains were picked out. The head capsules were slide mounted in Hydro-Matrix[®], or dehydrated in 100% ethanol and mounted in Euparal[®]. Identification was performed under a compound microscope at 400× magnification, with reference to Brooks et al.^[9], Wiederholm^[28], and an on-line photographic guide by Walker (<http://www.paleolab.ca/wwwguide/>). Most of the specimens were identified to genus level, and, in some cases, to species-morphotype level. Fragments that consisted of more than half the mentum were counted as a whole head capsule, fragments that consisted of half the mentum were counted as half a head capsule, and smaller fragments were excluded. A minimum of 50 head capsules was counted per sample, enough to provide reliable environmental inferences^[29].

The chironomid percentage diagram was constructed using the computer program TGView v. 2.0.2^[30]. Zones, defined by major changes in the composition of chironomid fauna, were identified by constrained incremental sum-of-squares (CONISS) cluster analysis^[31]. The statistical significance of these zones was evaluated by a broken stick model^[32]. Palaeosalinity was estimated for each fossil assemblage using a chironomid-salinity transfer function for Tibetan Plateau lakes developed by Zhang et al.^[18]. This calibration data set was based on surface-samples from 38 lakes on the Tibetan Plateau, spanning a modern salinity (TDS) range of 0.24–56.59 g/L. The Weighted Averaging-Partial Least Square (WA-PLS) TDS inference model used in this study has a coefficient of determination (R^2) of 0.77, a root mean square error of prediction (RMSEP) of 0.3082 and a maximum bias of 0.5317. The WA-PLS model was implemented using the computer program C2 v. 1.5.1^[33]. The same program was also used to derive sample-specific error estimates for the reconstructed salinities from Suga Lake. The wavelet analysis was performed using the computer program Matlab v. 7.4.0^[34].

2 Results and discussion

2.1 Chironomid assemblages

In all, five chironomid taxa were recorded from the 95 core samples: *Psectrocladius barbimanus*-type, *Orthocladus/Cricotopus*, *Procladius*, *Psectrocladius sordidellus*-type and *Chironomus anthracinus*-type. Most of these taxa are common in Tibetan Plateau lakes with TDS > 10 g/L, except *Chironomus anthracinus*-type, which was not in the training set. However, given the only occurrence of *Chironomus anthracinus*-type in the sequence at depth 52.6 cm, it is not shown in the stratigraphic diagram (Figure 2) and was omitted from the zonation analysis. Three major zones and nine subzones were distinguished based on a cluster analysis of the assemblage. All these zones and subzones were assessed to be statistically significant by the broken stick model.

Zone SG-Ch1 (268.4–130.0 cm, 990–1550 AD). This zone was largely dominated by *Orthocladus/Cricotopus* (72.2% of the fauna), but there was also a portion of *Psectrocladius barbimanus*-type (17.8%). The *Psectrocladius sordidellus*-type was present at a low percentage (6.7%), while *Procladius* only sporadically occurred. Generally, the variations in chironomid assemblages in this zone seemed rather slight except for the short section around 234.4 cm (1210 AD). SG-Ch1 was divided into three subzones (SG-Ch1a, SG-Ch1b

and SG-Ch1c).

On one hand, the species assemblage of SG-Ch1a (268.4–240.5 cm, 990–1200 AD) was similar to that of SG-Ch1c (228.8–130.0 cm, 1230–1550 AD), characterized by the overwhelming dominance of *Orthocladus/Cricotopus* at an abundance of 91.5% and 69.5%, respectively. *Psectrocladius barbimanus*-type was the second dominant taxon in SG-Ch1c (21.4%). *Psectrocladius sordidellus*-type appeared sporadically in SG-Ch1a, and was present in a relatively low percentage of 6.7% in SG-Ch1c. The abundance and occurrence of *Procladius* were both quite low in SG-Ch1a and SG-Ch1c. On the other hand, it was the relatively high abundance of *Psectrocladius sordidellus*-type (23.1%) and *Procladius* (19.4%) that made the SG-Ch1b (240.5–228.8 cm, 1200–1230 AD) distinct from the other two subzones. Specifically, *Procladius* reached its greatest abundance (35.8%) throughout the entire sequence at the depth of 2.34 m (1210 AD).

Zone SG-Ch2 (130.0–22.9 cm, 1550–1880 AD). This zone was distinguished by a dramatic increase in *Psectrocladius sordidellus*-type (26.7%). *Orthocladus/Cricotopus* declined to levels below 40%, although remained the predominant taxon (39.4%). *Psectrocladius barbimanus*-type was still an important element of the fauna (28.7%). *Procladius* showed its highest occur-

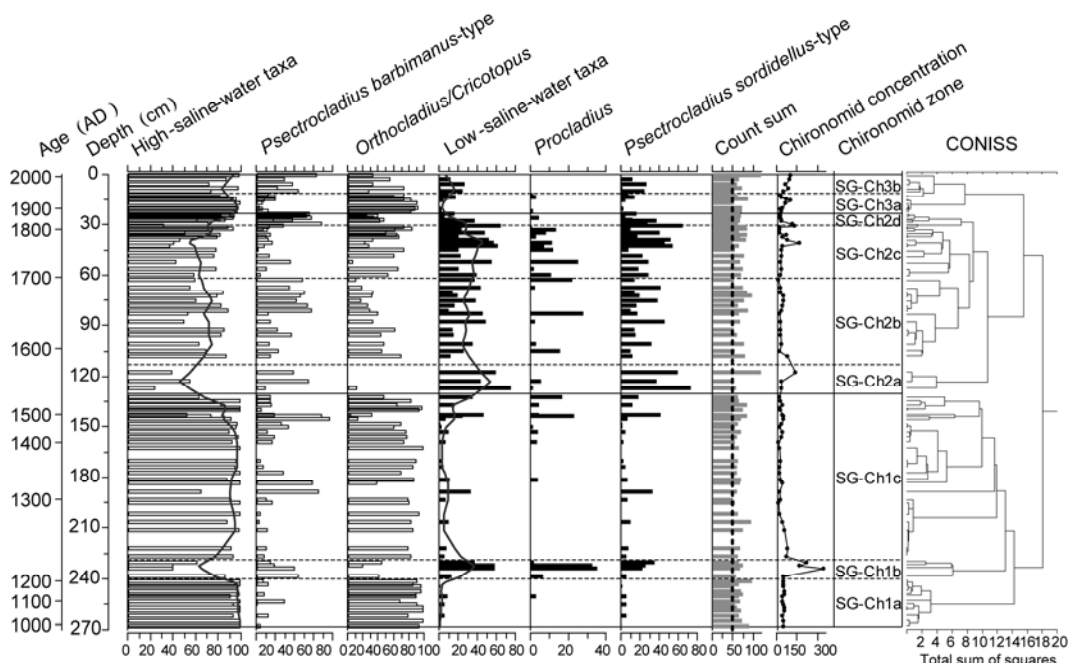


Figure 2 Chironomid stratigraphy of Suga Lake. Chironomid taxa are given as percentages of the total number of head capsules (hc), the count sum in number of hc per sample, and the chironomid concentration in number of hc per gram dry sediment.

rence during this zone, and its percentage moderately increased as well (4.9%). Comparing to SG-Ch1, the chironomid assemblages fluctuated much more considerably in this zone, which could be divided into four subzones.

In subzone SG-Ch2a (130.0–112.8 cm, 1550–1590 AD) and SG-Ch2c (61.7–30.4 cm, 1700–1820 AD), *Psectrocladius sordidellus*-type appeared at relatively high levels, becoming the most abundant taxon in SG-Ch2a (57.3%) for the first time in all the subzones, and the second most abundant in SG-Ch2c (28.5%). Additionally, SG-Ch2c was marked by consistently relatively high values of *Procladius*, with an average percentage of 6.6%. The abundance of *Orthocladius/Cricotopus* decreased drastically to 4.6% in SG-Ch2a. And *Psectrocladius barbimanus*-type had only an abundance of 13.6% in SG-Ch2c. However, distinct from SG-Ch2a and SG-Ch2c, *Orthocladius/Cricotopus* resumed its dominance in SG-Ch2b (112.8 cm–61.7 cm, 1590–1700 AD) (37.3%). Meanwhile, *Psectrocladius barbimanus*-type increased to a level just slightly lower than *Orthocladius/Cricotopus* (34.7%). *Psectrocladius sordidellus*-type appeared at a smaller percentage than that in SG-Ch2a and SG-Ch2c (22.2%). *Procladius* showed extremely variable abundances in this subzone, with three readily discernible high values greater than 15% and other zero or low values. Similar to SG-Ch2b, SG-Ch2d (30.4–22.9 cm, 1820–1880 AD) was also characterized by dominance of *Psectrocladius barbimanus*-type (49.3%) and *Orthocladius/Cricotopus* (32.8%). *Psectrocladius sordidellus*-type appeared at relatively low abundance (17.1%) and underwent a sharp fall across this subzone, while *Procladius* was present for the only time at 0.26 m.

Zone SG-Ch3 (22.9–0 cm, 1880–2000 AD). This zone was defined by the restored clear dominance of *Orthocladius/Cricotopus* (68.0%), but *Psectrocladius barbimanus*-type also made up a significant portion (23.2%). The abundance of *Psectrocladius sordidellus*-type declined to 8.2%, and *Procladius* only occurred sporadically with an extremely low percentage (0.5%). SG-Ch3 was divided into two subzones.

SG-Ch3a (22.9–11.2 cm, 1880–1960 AD) was overwhelmingly dominated by *Orthocladius/Cricotopus* (81.8%) but there were also some numbers of *Psectrocladius barbimanus*-type (12.4%). *Psectrocladius sordi-*

dellus-type decreased in abundance to 4.9%, and *Procladius* was only present in three samples. SG-Ch3b (11.2–0 cm, 1960–2000 AD) was distinguished by a steep fall of *Orthocladius/Cricotopus* (45.9%) and a simultaneous rise in *Psectrocladius barbimanus*-type (40.4%). The abundance of *Psectrocladius sordidellus*-type slightly increased to 13.6% but showed a declining trend towards the end of the subzone. In addition, *Procladius* was absent from SG-Ch3b.

2.2 Comparison of chironomid-based salinity records with other proxy data

Referring to the salinity optima of taxa in the Tibetan Plateau training set^[18] and the relevant ecological knowledge from the literature^[17,35], the four major chironomid taxa identified from SG031 were found to respond sensitively to changes in lake salinity. *Psectrocladius barbimanus*-type and *Orthocladius/Cricotopus* are indicative of relatively high-saline waters, whereas *Procladius* and *Psectrocladius sordidellus*-type are indicative of relatively low-saline waters. The salinity preferences of these taxa were confirmed by chironomid assemblage analysis of two modern surface samples from Sugan Lake^[19]. Therefore, overall variation in the chironomid fauna throughout the sequence can be generalized as changes in relative percentages of high-saline-water taxa (HSW_{ch} , %) and low-saline-water taxa (LSW_{ch} , %) (Figure 3), indicating palaeosalinity fluctuations and ultimately, effective moisture evolution.

The chironomid-inferred salinities (Sal_{ch} , g/L) for the last millennium (Figure 3) ranged between 23.0–53.4 with a mean value of 42.0 and an average error of ± 2.0 . The time series was divided roughly into three main stages when salinities were high (990–1550 AD and 1840–2000 AD) or low (1550–1840 AD).

Studies of modern process have shown that carbonate contents ($CaCO_3$) and carbonate oxygen isotope values ($\delta^{18}O_{carb}$) of Sugan Lake sediments were both good indicators for effective moisture changes in the catchment area^[21]. Therefore, we compared the Sal_{ch} and LSW_{ch} data with $CaCO_3$ and $\delta^{18}O_{carb}$ data to examine the validity of the chironomid-based salinity and effective moisture reconstruction from Sugan Lake. As shown in Figure 4, the Sal_{ch} and LSW_{ch} curves agree closely with the $CaCO_3$ and $\delta^{18}O_{carb}$ curves by visual inspection. Furthermore, the correlation coefficients of Sal_{ch} and $\delta^{18}O_{carb}$, and LSW_{ch} and $CaCO_3$ were both significant at

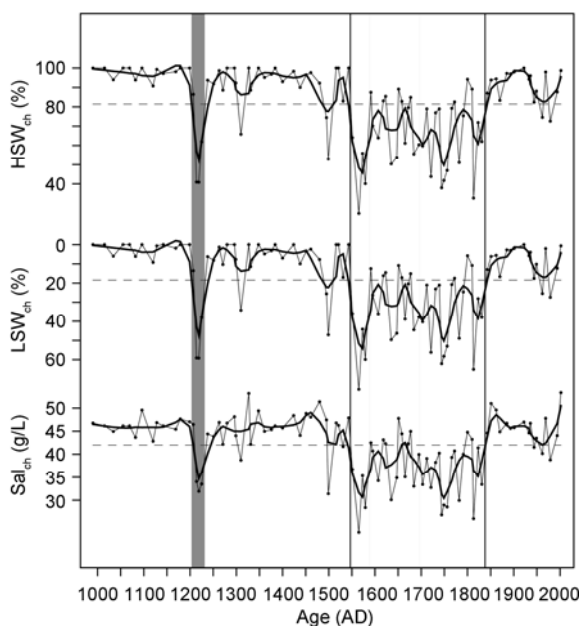


Figure 3 Percentages of high-saline-water taxa (HSW_{ch}) and low-saline-water taxa (LSW_{ch}), and chironomid-inferred salinities at Sugan Lake during the past millennium. Thick solid lines indicate LOESS smoothers (span = 0.95). Dash lines indicate averages of series. Inferred wet event is marked by shaded column and dry event by dotted column.

the 95% level, and those of Sal_{ch} and $CaCO_3$, and LSW_{ch} and $\delta^{18}O_{carb}$ were significant at 99% level. After removal of high-frequency components by a low-pass filter, it was evident that all four time series shared a common feature on the multi-centennial scale, namely a relatively humid LIA from the late 15th century to early 19th century (Figure 4). In addition, preliminary results from pollen analysis demonstrate that the pollen accumulation rate dramatically increased during the LIA, implying the prevalence of humid conditions during that interval¹⁾. Consequently, other physical, geochemical, and biological proxies from the same core corroborated our chironomid-based salinity reconstruction. This demonstrates that chironomid analysis can reliably reconstruct the effective moisture evolution in the Sugan Lake catchment over the past millennium.

2.3 Effective moisture evolution in the Sugan Lake catchment during the past millennium

According to the chironomid stratigraphy (Figure 2) and the chironomid-based salinity records (Figure 3), the effective moisture evolution in the Sugan Lake catchment was broadly divided into three periods at the

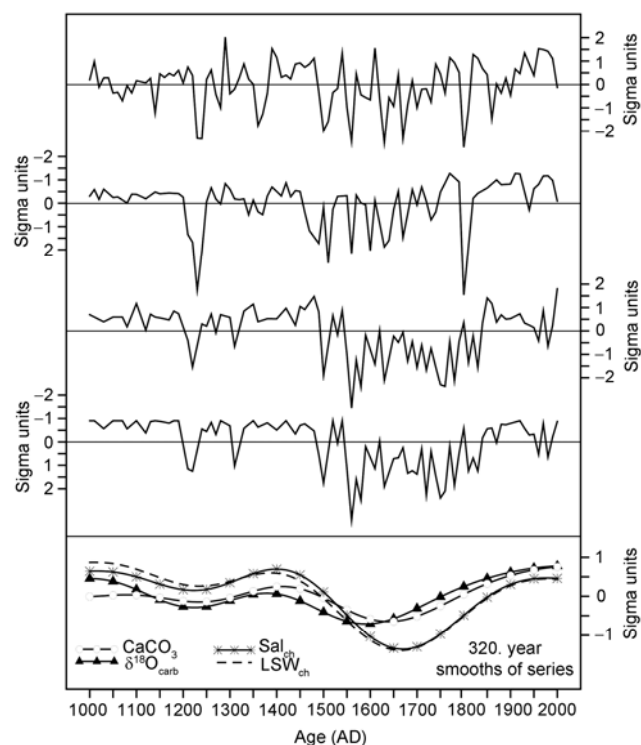


Figure 4 Comparison of chironomid inferred salinity (Sal_{ch}) and low-saline-water taxa (LSW_{ch}) data with carbonate content ($CaCO_3$) and carbonate oxygen isotope ($\delta^{18}O_{carb}$) data derived from the same core SG031. All series have been standardized. Smooths were generated using a 320-year low-pass filter^[36].

multi-centennial scale. (1) 990–1550 AD. This period was characterized by the overwhelming predominance of HSW_{ch} (90.5%), the sporadic presence of LSW_{ch} , and the high value of Sal_{ch} , which together indicate a low inflow/evaporation ratio and thus an arid climate in the catchment area. Previous works have proposed that there was a warm interval from the 9th century to 12th century in ANC^[37], largely coincident with the Medieval Warm Period (MWP) in China^[38]. Therefore, the catchment area probably experienced a warm and dry climate over this period. (2) 1550–1840 AD. This stage was distinguished by a significantly increased LSW_{ch} (34.2%) and generally the lowest Sal_{ch} within the whole sequence, suggesting that a sharp rise in the inflow/evaporation ratio occurred and relatively wet climatic conditions prevailed during this interval. Roughly synchronous with the so-called LIA in China (1400–1920 AD)^[38], the humid period we identified here was probably characterized by a cold temperature regime as well.

1) Zhang K. Personal communication.

(3) 1840–2000 AD. This stage was marked once more by a clear dominance of HSW_{ch} (90.8%) and a persistently higher Sal_{ch} than in the preceding interval, indicating the re-establishment of highly saline conditions and thus decreased effective moisture in the catchment area. Previous studies suggest that the Tibetan Plateau was highly sensitive to global warming^[39,40] and, therefore, the implication that a warm and dry climate prevailed throughout this period once again.

On the decadal to centennial time scale, the chironomid-based salinity records document two remarkable climatic events. (1) A relatively wet oscillation occurred in 1200–1230 AD, interrupting the generally dry period (990–1550 AD). This ~30-year effective moisture anomaly was marked by an abrupt increase in LSW_{ch} (1.8%–42.5%) and a considerable decline in Sal_{ch} . The rapid rise in the inflow/evaporation ratio may represent a multi-decadal humid event against a long-term, arid climatic context. This wet interval is not only reflected in other proxy data from SG03I (Figure 4), but is also consistent with a period of high precipitation (1207–1260 AD) in Delingha (37°22'N, 97°22'E) reconstructed from tree rings from northeastern part of Qaidam Basin^[41]. The Delingha precipitation record provides some valuable information concerning climatic conditions in the headwater area of the Sugan Lake drainage basin. However, this humid event is neither documented in the tree-ring inferred precipitation record from Dulan (36°10'N, 98°00'E) to the southeast of Delingha^[42], nor in the ice-core accumulation record from Guliya (35°12'N, 81°30'E) on the northwestern Tibetan Plateau^[43]. Therefore, its climatic significance for the wider region still remains to be tested by more high-resolution palaeo-data. (2) A comparatively dry oscillation occurred in 1590–1700 AD, punctuating the generally humid LIA. This ~110-year effective moisture anomaly is indicated by the increase in HSW_{ch} (46.1%–72.0%) and moderately increased Sal_{ch} . The intensity of this dry event was not as great as that of the two arid periods (990–1550 AD, 1840–2000 AD) revealed at the multi-centennial scale. Cross-site comparison shows that the occurrence of this relatively arid interval is in general agreement with a period of low precipitation (1634–1741 AD) indicated by Delingha tree-ring record^[41], and with a dry period 1580–1710 AD suggested by high microparticle concentrations in the ice-core from Dunde (38°06'N, 96°24'E) just ~120

km away from Delingha^[44]. In Qinghai Lake (37°N, 100°E) to the east, Zhang et al.^[45] also reported an arid interval from 1560 AD to 1650 AD. However, the relatively dry event identified here is not documented in the palaeoclimatic records from Guliya^[43] and Bosten Lake (42°05'N, 87°03'E)^[5], which are located in the western and central part of ANC, respectively. Therefore, we postulate that the decadal to centennial wet and dry events revealed by our chironomid-based salinity reconstruction from Sugan Lake are just of local climatic significance, and could be related to moisture anomalies in the headwater area of its drainage basin.

As far as the trends in the inferred salinity time series are concerned, it is evident that the magnitude of salinity fluctuation was greater, and the frequency higher, in the relatively humid LIA (1550–1840 AD) than in the preceding and following dry periods (Figure 3), implying a highly unstable LIA climate in the catchment area of Sugan Lake. In particular, the standard deviation (SD) of inferred salinities indicates a significant rise to 6.3 g/L from 4.7 g/L. And the increased frequency of salinity fluctuations during the LIA is clearly demonstrated by the considerably higher values of the real Morlet wavelet coefficients over the 20 to 100-year band (Figure 5(a)). Morlet wavelet transform of the $\delta^{18}O_{carb}$ time series derived from SG03I shows a similar pattern (Figure 5(b)). In Delingha, the magnitude of variation in reconstructed precipitation increased to 30 mm between 1430 and 1850 AD, from 15 mm between 1000 and 1430 AD, and declined after 1850 AD^[41]. A recent tree-ring based 1436-year reconstruction of soil moisture from northeastern Qaidam Basin indicates that greater high-frequency and low-frequency variations were apparent during the LIA, while fluctuations were damped over the period before 1500 AD^[46]. Furthermore, it is noteworthy

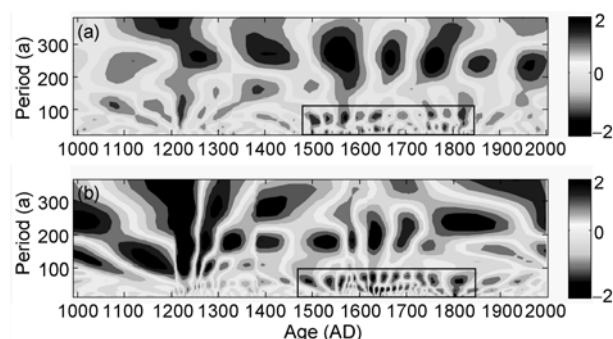


Figure 5 The Morlet wavelet transform of Sal_{ch} time series (a) and $\delta^{18}O_{carb}$ time series (b). Solid line rectangles indicate increased high-frequency fluctuations during the LIA.

that increased climate instability during the LIA was also reflected in the Guliya accumulation record^[43]. The SD of accumulation reached 51.6 mm in the generally humid period 1500–1830 AD, whereas the magnitude of variation in accumulation was comparatively low during the dry period 900–1500 AD (SD = 36 mm). In view of this, these results suggest that the unstable LIA climate revealed by our chironomid-based salinity reconstruction from Sugan Lake might have a wider regional significance, rather than only prevailing on the northeastern Tibetan Plateau.

2.4 Comparison of moisture evolution in the westerly-dominated ANC and monsoonal China during the past millennium

The effective moisture evolution in the Sugan Lake catchment during the past millennium has been reliably reconstructed using chironomid analysis, and features a generally humid LIA (Figure 6(c), (d)). The available palaeo-moisture records from other sites in the westerly-dominated ANC can be summarized as follows. Proxy records from Guliya (western Kunlun Mts.)^[43] and Bosten Lake (Tianshan Mts.)^[5] suggest that precipitation was high in the mountains during the LIA (Figure

6(a), (b)). Accordingly, the discharge of big endorheic rivers such as those on the fringe of Tarim Basin increased^[47,48] and the areas of terminal lakes in the desert expanded, for example, at Aibi Lake (44°53'N, 83°00'E)^[49] and Juyan Lake (42°06'N, 101°15'E)^[50]. The groundwater recharge rates in the Badain Jaran desert (39°20'–41°30'N, 99°48'–104°14'E) also increased in the LIA^[51]. In addition, palaeoclimate reconstructions from arid central Asia to the west of ANC also suggested a prevalence of wet conditions in the LIA^[37,52,53]. Taken together, all these records demonstrate that the generally humid LIA climate documented in the chironomid-based salinity records from Sugan Lake is at least of an ANC-wide regional significance. However, apart from the decade-scale accumulation series from Guliya, the climatic instability during the LIA evident in the Sugan Lake catchment has not been detected in previous records due to insufficient temporal resolution.

The precipitation variability in monsoonal China over the last 1000 years has been well-recorded in precisely-dated cave deposits^[54,55] (Figure 6(e), (f)) and historical documents^[56] (Figure 6(g)). For this region, we can roughly divide the LIA into two climatically distinct

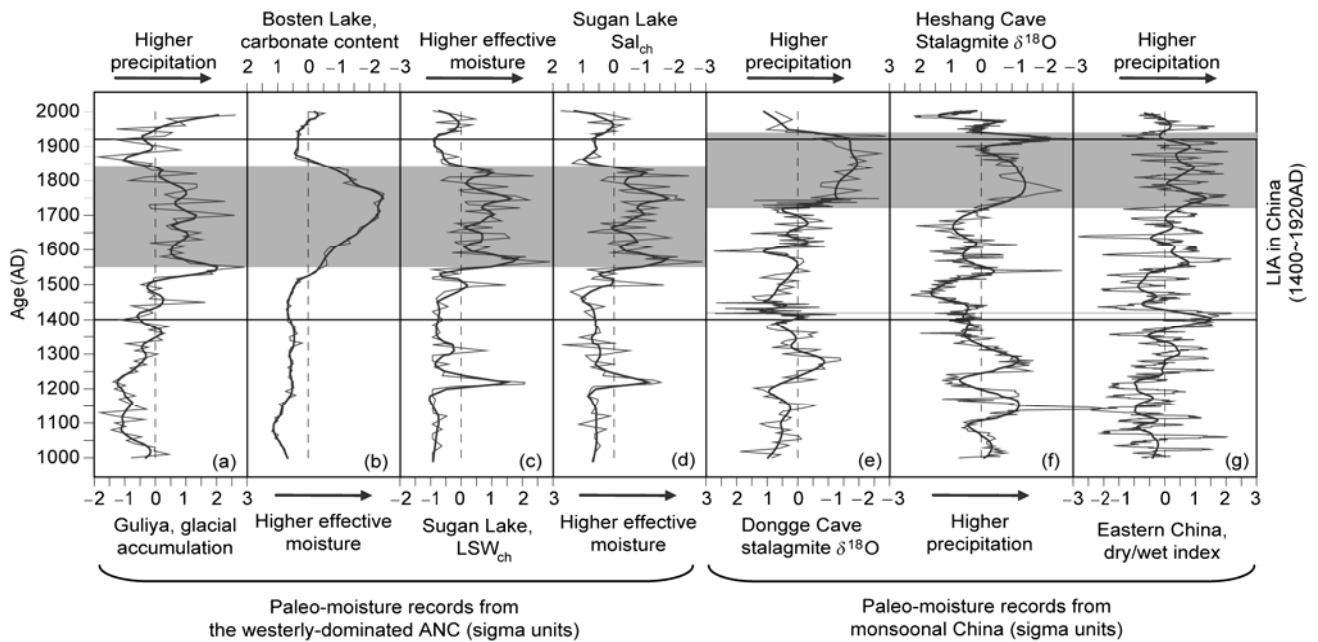


Figure 6 Comparison between moisture evolution in the westerly-dominated ANC and that in monsoonal China over the last millennium. (a) Guliya, glacial accumulation record^[43]; (b) Bosten Lake, carbonate content record^[5]; (c) Sugan Lake, LSW_{ch} record; (d) Sugan Lake, Sal_{ch} record; (e) Dongge Cave, stalagmite $\delta^{18}O$ record^[54]; (f) Heshang Cave, stalagmite $\delta^{18}O$ record^[55]; (g) Eastern China, dry/wet index record^[56]. All series have been standardized. Thick solid lines indicate LOESS smoothers (span = $10\% \times N$, where N stands for number of samples). Wet periods within the LIA are marked by shaded band and dry periods by dotted band. The general timing of the LIA in China (1400–1920 AD) follows Yang et al.^[38].

periods: the first half marked by relatively low precipitation and thus a relatively weak Asian monsoon; the second half characterized by positive precipitation anomalies and an intensified Asian monsoon. The transition of the climatic regime from relatively dry to wet occurred around the mid-17th century. Comparison of the effective moisture (or precipitation) variability in the westerly-dominated ANC with that in monsoonal China during the past millennium, focusing on the LIA, demonstrates that the timing of moisture evolution was significantly different between the two regions (Figure 6). The rise of effective moisture in ANC commenced in the early 16th century whereas, in monsoonal China, the humid period started from ~1700 AD onwards. The termination of the generally wet interval in ANC occurred around 1840 AD, while the proxy data from monsoonal China suggest relatively high precipitation rates at that time. On the basis of these findings, we conclude that the “out-of-phase” relationship between moisture evolution in ANC and monsoonal China suggested by Chen et al.^[2] for the Holocene probably also pertained during the last millennium.

Several possible mechanisms for the relatively humid conditions during the LIA over the westerly-dominated ANC are possible. First, the southward shift of the westerlies and the stronger pole-equator thermal gradient, associated with low temperatures during the LIA, could have resulted in an increase of cyclonic activity over the mid-latitudes and thus more precipitation^[57,58]. Second, the predominantly negative NAO winter index during the LIA^[59] could have led to an increase in precipitation at mid-latitudes of continental Asia. This inverse association was suggested by statistical analyses of meteorological data from relevant hydro-climatic stations^[60]. Third, the reduction in evapotranspiration due to the cold LIA climate may also have contributed to the increased effective moisture in ANC. However, to test and validate these and other possible explanations, more modeling efforts are required.

3 Conclusions

(1) Decade-scale analysis of the chironomid fauna in the upper 2.9 m of the annually laminated sediments of core SG03I from Sugan Lake revealed significant variations in HSW_{ch} and LSW_{ch} during the last millennium. The chironomid stratigraphy can be divided into three major

zones and nine sub-zones. Chironomid-based salinity records are consistent with $CaCO_3$ and $\delta^{18}O_{carb}$ data from the same core in terms of general trends and the magnitude and frequency of the variability, confirming the reliability of the effective moisture reconstruction by chironomid analysis for the Sugan Lake catchment.

(2) The chironomid-based salinity records revealed the effective moisture evolution in the catchment of Sugan Lake during the past millennium. From 990 AD to 1550 AD, the climate was generally arid, as suggested by the predominance of HSW_{ch} and the high value of Sal_{ch} . During the period 1550–1840 AD, LSW_{ch} considerably increased and Sal_{ch} dramatically declined, indicating relatively humid conditions. This wet period was roughly synchronous with the cold LIA in China. After 1840 AD, the HSW_{ch} and Sal_{ch} both rose to a high level, implying that the dry climate prevailed in this area once again. At the decadal to centennial scale, a wet event at around 1200–1230 AD and a comparably dry event at around 1590–1700 AD were documented by the chironomid-based salinity reconstruction. In addition, the climate became more unstable during the relatively humid LIA, as reflected by the greater magnitude and higher frequency of salinity fluctuations during that period.

(3) The generally humid LIA climate documented, in the chironomid-based salinity reconstruction from Sugan Lake, was of an ANC-wide regional significance, whereas the decadal to centennial wet and dry events were only associated with moisture anomalies in the headwater area of the Sugan Lake drainage basin. The increased climatic instability during the LIA revealed by our chironomid record might have a wider regional importance, rather than being limited to the northeastern Tibetan Plateau.

(4) The moisture evolution in the westerly-dominated ANC during the last millennium had an “out-of-phase” relationship with that in monsoonal China at the multi-centennial scale. The relatively humid LIA climate in ANC can be plausibly attributed to the increased precipitation resulting from equatorward westerlies and negative NAO index, and the reduced evapotranspiration due to lower temperatures.

Part of the work was undertaken at NHM through a CSC studentship to JHC. We thank Prof. Zheng Jingyun and Ge Quansheng, IGSNRR, CAS, for kindly providing the dry/wet index data of eastern China. The manuscript has also benefited from invaluable comments of two anonymous reviewers.

- 1 Moberg A, Sonechkin D M, Holmgren K, et al. Highly variable Northern Hemisphere temperatures reconstructed from low- and high-resolution proxy data. *Nature*, 2005, 433: 613–617
- 2 Chen F H, Yu Z C, Yang M L, et al. Holocene moisture evolution in arid central Asia and its out-of-phase relationship with Asian monsoon history. *Quat Sci Rev*, 2008, 27: 351–364
- 3 Shi Y, Shen Y, Kang E, et al. Recent and future climate change in Northwest China. *Clim Change*, 2007, 80: 379–393
- 4 Yang B, Braeuning A, Shi Y, et al. Evidence for a late Holocene warm and humid climate period and environmental characteristics in the arid zones of northwest China during 2.2–1.8 kyr BP. *J Geophys Res*, 2004, doi: 10.1029/2003JD003787
- 5 Chen F H, Huang X Z, Zhang J W, et al. Humid Little Ice Age in and central Asia documented by Bosten Lake, Xinjiang, China. *Sci China Ser D-Earth Sci*, 2006, 49: 1280–1290
- 6 Walker I R. Overview of fossil Chironomids. In: Elias S A, ed. *Encyclopedia of Quaternary Science*. Amsterdam: Elsevier, 2007. 360–366
- 7 Walker I R. Chironomidae (Diptera) in paleoecology. *Quat Sci Rev*, 1987, 6: 29–40
- 8 Ferrington L C. Global diversity of non-biting midges (Chironomidae; Insecta-Diptera) in freshwater. *Hydrobiologia*, 2008, 595: 447–455
- 9 Brooks S J, Langdon P G, Heiri O. The Identification and Use of Palaearctic Chironomidae Larvae in Palaeoecology. QRA Technical Guide No. 10. London: Quat Res Assoc, 2007
- 10 Walker I R. Midges: Chironomidae and related Diptera. In: Smol J P, Birks H J B, Last W M, eds. *Tracking Environmental Change Using Lake Sediments. Volume 4: Zoological Indicators*. Dordrecht: Kluwer Academic Publishers, 2001. 43–66
- 11 Heinrichs M L, Walker I R. Fossil midges and palaeosalinity: potential as indicators of hydrological balance and sea-level change. *Quat Sci Rev*, 2006, 25: 1948–1965
- 12 Fritz S. Deciphering climatic history from lake sediments. *J Paleolimnol*, 2008, 39: 5–16
- 13 Verschuren D, Laird K R, Cumming B F. Rainfall and drought in equatorial east Africa during the past 1,100 years. *Nature*, 2000, 403: 410–414
- 14 Verschuren D, Cumming B F, Laird K R. Quantitative reconstruction of past salinity variations in African lakes: assessment of chironomid-based inference models (Insecta : Diptera) in space and time. *Can J Fish Aquat Sci*, 2004, 61: 986–998
- 15 Eggermont H, Heiri O, Verschuren D. Fossil Chironomidae (Insecta : Diptera) as quantitative indicators of past salinity in African lakes. *Quat Sci Rev*, 2006, 25: 1966–1994
- 16 Heinrichs M L, Walker I R, Mathewes R W. Chironomid-based paleosalinity records in southern British Columbia, Canada: A comparison of transfer functions. *J Paleolimnol*, 2001, 26: 147–159
- 17 Walker I R, Wilson S E, Smol J P. Chironomidae (Diptera)-Quantitative paleosalinity indicators for lakes of western Canada. *Can J Fish Aquat Sci*, 1995, 52: 950–960
- 18 Zhang E, Jones R, Bedford A, et al. A chironomid-based salinity inference model from lakes on the Tibetan Plateau. *J Paleolimnol*, 2007, 38: 477–491
- 19 Chen J H, Chen F H, Zhang E L, et al. A preliminary study on chironomid-based salinity reconstruction for Sugan Lake in the last millennium (in Chinese). *Quat Sci*, 2008, 28: 338–344
- 20 Zhou A F, Chen F H, Qiang M R, et al. The discovery of annually laminated sediments (varves) from shallow Sugan Lake in inland arid China and their paleoclimatic significance. *Sci China Ser D-Earth Sci*, 2007, 50: 1218–1224
- 21 Zhou A F. Varve chronology and late Holocene environmental changes in Sugan Lake, Northern Qaidam Basin (in Chinese). Dissertation for Doctoral Degree. Lanzhou: Lanzhou University, 2007
- 22 Wang S M, Dou H S. *Lakes in China* (in Chinese). Beijing: Science Press, 1998. 485, 501
- 23 Qiang M R, Chen F H, Zhang J W, et al. Climatic changes documented by stable isotopes of sedimentary carbonate in Lake Sugan, northeastern Tibetan Plateau of China, since 2 ka BP. *Chinese Sci Bull*, 2005, 50: 1930–1939
- 24 Holmes J A, Zhang J W, Chen F H, et al. Paleoclimatic implications of an 850-year oxygen-isotope record from the northern Tibetan Plateau. *Geophys Res Lett*, 2007, 34, doi: 10.1029/2007gl032228
- 25 Zhang J, Holmes J A, Chen F, et al. An 850-year ostracod-shell trace-element record from Sugan Lake, northern Tibetan Plateau, China: Implications for interpreting the shell chemistry in high-Mg/Ca waters. *Quat Int*, 2008, doi: 10.1016/j.quaint.2008.05.003
- 26 Gao Y X. *Some Questions About the East Asian Monsoon* (in Chinese). Beijing: Science Press, 1962
- 27 Morrill C, Overpeck J T, Cole J E. A synthesis of abrupt changes in the Asian summer monsoon since the last deglaciation. *Holocene*, 2003, 13: 465–476
- 28 Wiederholm T. Chironomidae of the Holarctic region. Keys and diagnoses. Part 1. Larvae. *Entomologica Scandinavica Supplement*, 1983, 19: 1–457
- 29 Larocque I. How many chironomid head capsules are enough? A statistical approach to determine sample size for palaeoclimatic reconstructions. *Palaeogeogr Palaeoclimatol Palaeoecol*, 2001, 172: 133–142
- 30 Grimm E C. *TGView version 2.0.2*. Springfield: Illinois State Museum, Research and Collections Center. 2004
- 31 Grimm E C. *Tilia version 2.0.b.4*. Springfield: Illinois State Museum, Research and Collections Center. 1993
- 32 Bennett K D. Determination of the number of zones in a biostratigraphical sequence. *New Phytol*, 1996, 132: 155–170
- 33 Juggins S. *C2 version 1.5: Software for ecological and palaeoecological data analysis and visualisation*. Newcastle upon Tyne: University of Newcastle. 2007
- 34 Matlab version 7.4.0. Natick, Massachusetts: The MathWorks Inc. 2007

- 35 Heinrichs M L, Wilson S E, Walker I R, et al. Midge- and diatom-based palaeosalinity reconstructions for Mahoney Lake, Okanagan Valley, British Columbia, Canada. *Int J Salt Lake Res*, 1997, 6: 249–267
- 36 Mann M E. On smoothing potentially non-stationary climate time series. *Geophys Res Lett*, 2004, 31: 710–713
- 37 Yang B, Wang J, Braeuning A, et al. Late Holocene climatic and environmental changes in arid central Asia. *Quat Int*, 2008, doi: 10.1016/j.quaint.2007.11.020
- 38 Yang B, Braeuning A, Johnson K R, et al. General characteristics of temperature variation in China during the last two millennia. *Geophys Res Lett*, 2002, 29: 38–31
- 39 Liu X D, Chen B D. Climatic warming in the Tibetan Plateau during recent decades. *Int J Climatol*, 2000, 20: 1729–1742
- 40 Gou X, Chen F, Jacoby G, et al. Rapid tree growth with respect to the last 400 years in response to climate warming, northeastern Tibetan Plateau. *Int J Climatol*, 2007, 27: 1497–1503
- 41 Shao X M, Huang L, Liu H B, et al. Reconstruction of precipitation variation from tree rings in recent 1000 years in Delingha, Qinghai. *Sci China Ser D-Earth Sci*, 2005, 48: 939–949
- 42 Zhang Q B, Cheng G D, Yao T D, et al. A 2,326-year tree-ring record of climate variability on the northeastern Qinghai-Tibetan Plateau. *Geophys Res Lett*, 2003, 30, doi: 10.1029/2003gl017425
- 43 Yao T D, Thompson L G, Qin D H, et al. Variations in temperature and precipitation in the past 2000 a on the Xizang (Tibet) Plateau—Guliya ice core record. *Sci China Ser D-Earth Sci*, 1996, 39: 425–433
- 44 Liu C P, Yao T D, Thompson L G, et al. Variation in microparticle concentrations preserved in the Dunde ice core and its relationship to dust storms and climate since the Little Ice Age. *J Glaciol Geocryol*, 1999, 21: 385–390
- 45 Zhang J W, Jin M, Chen F H, et al. High-resolution precipitation variations in the Northeast Tibetan Plateau over the last 800 years documented by sediment cores of Qinghai Lake. *Chinese Sci Bull*, 2003, 48: 1451–1456
- 46 Yin Z Y, Shao X M, Qin N S, et al. Reconstruction of a 1436-year soil moisture and vegetation water use history based on tree-ring widths from Qilian junipers in northeastern Qaidam Basin, northwestern China. *Int J Climatol*, 2008, 28: 37–53
- 47 Liu B. *Climate Change in Southern Tarim Basin*. Tokyo: Ancient and Present-Day Bookstore, 1976
- 48 Yang X P, Zhu Z D, Jaekel D, et al. Late Quaternary palaeoenvironment change and landscape evolution along the Keriya River, Xinjiang, China: the relationship between high mountain glaciation and landscape evolution in foreland desert regions. *Quat Int*, 2002, 97-8: 155–166
- 49 Wu J L, Liu J J, Wang S M. Climatic change record from stable isotopes in Lake Aibi, Xinjiang during the past 1500 years (in Chinese). *Quat Sci*, 2004, 24: 585–590
- 50 Zhang Z K, Wang S M, Wu R J, et al. Environmental changes recorded by lake sediments from east Juyanhai Lake in inner Mongolia during the past 2600 years(in Chinese). *J Lake Sci*, 1998, 10: 44–51
- 51 Ma J Z, Li D, Zhang J W, et al. Groundwater recharge and climatic change during the last 1000 years from unsaturated zone of SE Badain Jaran Desert. *Chinese Sci Bull*, 2003, 48: 1469–1474
- 52 Sorrel P, Popescu S M, Head M J, et al. Hydrographic development of the Aral Sea during the last 2000 years based on a quantitative analysis of dinoflagellate cysts. *Palaeogeogr Palaeoclimatol Palaeoecol*, 2006, 234: 304–327
- 53 Kroonenberg S B, Abdurakhmanov G M, Badyukova E N, et al. Solar-forced 2600 BP and Little Ice Age highstands of the Caspian sea. *Quat Int*, 2007, 173: 137–143
- 54 Wang Y J, Cheng H, Edwards R L, et al. The Holocene Asian monsoon: Links to solar changes and North Atlantic climate. *Science*, 2005, 308: 854–857
- 55 Hu C Y, Henderson G M, Huang J H, et al. Quantification of Holocene Asian monsoon rainfall from spatially separated cave records. *Earth Planet Sc Lett*, 2008, 266: 221–232
- 56 Zheng J Y, Wang W C, Ge Q S, et al. Precipitation variability and extreme events in eastern China during the past 1500 years. *Terr Atmos Ocean Sci*, 2006, 17: 579–592
- 57 Magny M, Begeot C, Guiot J, et al. Contrasting patterns of hydrological changes in Europe in response to Holocene climate cooling phases. *Quat Sci Rev*, 2003, 22: 1589–1596
- 58 Raible C C, Yoshimori M, Stocker T F, et al. Extreme midlatitude cyclones and their implications for precipitation and wind speed extremes in simulations of the Maunder Minimum versus present day conditions. *Clim Dyn*, 2007, 28: 409–423
- 59 Chu G Q, Sun Q, Wang X H, et al. Snow anomaly events from historical documents in eastern China during the past two millennia and implication for low-frequency variability of AO/NAO and PDO. *Geophys Res Lett*, 2008, doi: 10.1029/2008gl034475
- 60 Aizen E M, Aizen V B, Melack J M, et al. Precipitation and atmospheric circulation patterns at mid-latitudes of Asia. *Int J Climatol*, 2001, 21: 535–556